Polymer Journal, Vol. 24, No. 7, pp 641—652 (1992)

Mono- and Multilayer Langmuir–Blodgett Films of Cellulose Tri-*n*-alkyl Esters Studied by Transmission Electron Microscopy

Takahiro ITOH, Yoshinobu TSUJII, Hidematsu Suzuki,*
Takeshi FUKUDA, and Takeaki MIYAMOTO

Institute for Chemical Research, Kyoto University, Uji, Kyoto 611, Japan
** Department of BioEngineering, Nagaoka University of Technology, Nagaoka, Niigata 940-21, Japan*

(Received October 9, 1991)

ABSTRACT: The mono- and multilayer Langmuir–Blodgett films of cellulose tri(n-decanoate) (CTD) and cellulose tri(*n*-octadecanoate) (CTO) were prepared and studied with their fine structures and layer thicknesses by transmission electron microscopy. CTD was found to give a *perfectly homogeneous* monolayer film. The observed values of the film thickness L and the limiting area A indicated that the alkyl side chains are nearly fully extended and closely packed. The π–A isotherm of this polymer (but not of CTO) exhibited a plateau region, which was interpreted in terms of a monolayer-to-bilayer transition. CTO also gave a homogeneous monolayer film, which was repeatedly transferred to give multilayer films with a homogeneous surface structure. The observed values of L and A suggested that the alkyl side chains in each layer are essentially extended, but in a somewhat poorly defined fashion as compared with those in the CTD film.

KEY WORDS Cellulose Esters / Monolayer Films / Multilayer Films / Homogeneous Films / Electron Microscopy /

Among the number of current technologies, the Langmuir–Blodgett (LB) technique is particularly useful for preparing molecular devices,[1,2] which often demand homogeneity of the film. Many techniques are used for studying the fine structure of surface monolayers.[3-7] Transmission electron microscopy (TEM) is a most powerful method to directly observe the fine structure (as well as the thickness) of LB films.[3,5] By this method, Uyeda *et al.*[3] found that a stearic acid monolayer, which shows a typical condensed-type surface pressure (π)–area (A) isotherm, is inhomogeneous with many holes, as opposed to the prevailing view.

In this paper, we have adopted the TEM technique to study the structure of the mono- and/or multilayer LB films of two ester derivatives of cellulose, cellulose tri(*n*-decanoate) (CTD) and cellulose tri(*n*-octadecanoate) (CTO). Many cellulose tri(*n*-alkyl) esters, including CTD, have already been studied by Kawaguchi *et al.*[4] in detail with respect to their surface and film properties, but the fine structure and thickness of those LB films have never been observed as yet. We will show that CTD and CTO, spread at the air/water interface and transferred onto a substrate at certain points of the π–A isotherm, form perfectly *homogeneous* monolayer films. To our knowledge, this is the first report (excepting preliminary reports from our group[7]) that has confirmed the homogeneity of a monolayer film by TEM. We will also report about a TEM study of the multilayer films prepared by repeatedly transferring the homogeneous sur-

face film of CTO.

EXPERIMENTAL

Materials

As a starting material, a commercial cellulose diacetate (Daicel Chem. Ind.) whose degree of substitution (DS) and viscosity-average degree of polymerization (DP) are 2.44 and *ca.* 200, respectively, was used. The acid chlorides used were *n*-decanoyl (extra pure) and *n*-octadecanoyl (chemical pure) chlorides. Pyridine (guaranteed grade) and the solvents, 1,4-dioxane and toluene, were dried over potassium hydroxide and metallic sodium, respectively. All reagents were distilled just before use.

Preparation of Cellulose Esters

The cellulose diacetate was treated with a 17% aqueous ammonia solution at room temperature for three days, followed by thorough washing and drying.[8] Completion of deacetylation was confirmed in terms of the disappearance of the 1750 cm^{-1} absorption band due to the ester carbonyl stretching mode. Amphiphilic triester samples, cellulose tri(*n*-decanoate) (CTD) and cellulose tri(*n*-octadecanoate) (CTO) were prepared by the acid chloride - pyridine procedure[8]: The regenerated cellulose (0.65 g, 4×10^{-3} mol-equivalent) was dispersed in 15 ml of 1,4-dioxane (for CTD) or toluene (for CTO), followed by the addition of pyridine (1.34 g, 1.7×10^{-2} mol). Then, each acid chloride (1.4×10^{-2} mol) diluted with an equal volume of the solvent was added dropwise. The reaction was carried out under reflux over 24 h. The reaction mixture was then poured into a methanol–water mixture (10 : 1 by volume), and the precipitate was separated by filtration and dried. These crude products were dissolved in tetrahydrofuran (THF), and the insoluble impurities were removed by centrifugation. The obtained supernatant solutions were poured into methanol (for CTD) or hot methanol (for CTO) to precipitate the desired esters. The precipitates were washed with methanol and dried *in vacuo*. After these procedures were repeated several times, the cellulose esters were obtained in pure form.

General Analyses

IR spectra of the films cast on NaCl disks from chloroform solutions of the cellulose derivatives were recorded on a JASCO FT/IR-8000 spectrophotometer. As for the regenerated cellulose, the KBr tablet method was applied. ^{1}H-nuclear magnetic resonance (NMR) spectra were recorded on a Varian VXR-200 spectrometer (200 MHz) in $CDCl_3$ (99% purity, Aldrich) at room temperature. Elemental analyses were carried out with respect to C and H.

Preparation of Monolayers and Surface Pressure Measurements

Monolayers were spread on a clean water surface in a Langmuir trough ($200 \times 500 \times 3$ mm^3), the temperature of which was kept constant by circulating thermostated water. The subphase water was purified by means of a Mitamura Riken model PLS-DFR automatic still, which consisted of a reverse-osmosis module, an ion-exchange column and a double distiller. Each sample was spread from its dilute solution (1×10^{-6}—1×10^{-7} mol-eq in ml) in 4-methyl-2-pentanone (MIBK, guaranteed grade), benzene or chloroform (both in spectrograde). After 30 min was allowed for the solvent to evaporate off, the monolayer was compressed at a constant speed of 12 cm^2 min^{-1}, and the surface pressure was measured, as a function of the area, by means of a film balance of a Whilhelmy type.

Film Transfer–Monolayer Films

For observing its surface structure, the monolayer was transferred, at several points of the π–A isotherm, from the water surface to a specimen copper grid (2.3 mm in diameter, 400 mesh) covered with a carbon film[9] (7 nm in thickness) in an ordinary way. Namely, the carbon film side of the grid placed strictly

parallel with the water surface was allowed to just touch the monolayer surface from the air side and then withdrawn by using an elevation apparatus with the hydrophobic side of the monolayer adhered on the carbon film. The area of the carbon grid was so small that a drop of water was lifted up together, which was removed off by use of filter paper. This procedure allowed a *single* layer (not a Y-type bilayer, see below) to be transferred. (It was recently suggested that an "overturning" of molecules after the deposition can occur in certain X-type films.[10] This is not the case with our system, as the below-mentioned observations of the thickness and fine structure of the films show.)

To prepare a specimen for the TEM observation of the film thickness, the substrate grid was pretreated as follows: A cellulose acetobutyrate micro-grid having many holes of several μm in diameter was stuck on a copper specimen grid (2.3 mm in diameter, 400 mesh), which was vacuum-coated with carbon and then with gold in order to protect it from an electron radiation damage. Thus modified micro-grid was stacked with a thin carbon film (7 nm) and then coated with platinum *in vacuo*,[5] followed by air-sputtering under a reduced pressure (10 Pa) just before use. Thus prepared grid was suspended vertically in the water of the trough prior to spreading the monolayer. At a desired point of compression, the suspended grid was drawn up at a speed of 1 mm min^{-1}. This procedure allowed for a *monolayer* to be transferred onto the platinum surface of the grid with its hydrophobic side outside.

Film Transfer–Multilayer Films

In order to prepare multilayer films, two kinds of techniques were used: a vertical dipping and horizontal lifting methods. In the former method, the plate was dipped in and out vertically to the water surface at a speed of 0.5—5 mm min^{-1}. In the latter method, the glass plate was brought down parallelly to the water surface until it just touched the monolayer and then lifted up at a speed of 3—0.5 mm min^{-1}. During the deposition, the surface pressure was kept constant at 10 mN m^{-1} (see below). The substrate with the built-up film was dried *in vacuo* after every deposition.

To check transferability, Pyrex glass plates with an area of 28×18 mm^2 and of 28×50 mm^2 were used for the horizontal and vertical deposition methods, respectively. To make the surface hydrophilic, the glass plates, washed with toluene, were sputtered with air under a reduced pressure (10 Pa). Substrates with a hydrophobic surface were prepared in the following way; a glass plate, which had been cleaned by dipping firstly in sulfuric acid containing a small amount of potassium permanganate and secondly in a 10% hydrogen peroxide solution followed by washing with pure water, was dipped in a 10 % toluene solution of trimethylchlorosilane (Nacalai Tesque, Inc.) for 1 hr and then washed with toluene.

By the horizontal lifting method, a multilayer film was transferred on the hydrophobic surfaces of both carbon and platinum films. The carbon film was vapor-deposited on the glass plate (24×18 mm^2) which was washed with toluene. After the deposition ($\pi = 10$ mN m^{-1}), the plate was immersed slowly in clean water, and the carbon film floating on the water with the sample on it was picked up with a copper grid (3 mm in diameter, 400 mesh). This sample was used for the observation of the surface film structure. On the other hand, for observation of the thickness, a multilayer was prepared as follows; platinum was vapor-deposited on the carbon-precoated glass plate used above. After monolayers were repeatedly transferred on the non-sputtered platinum surface at $\pi = 10$ mN m^{-1} by the horizontal lifting method, the plate was immersed slowly in clean water, and the platinum film with the multilayer floating on the water was picked up with a gold-coated

microgrid.

TEM Observations

The surface structure of the monolayers transferred on the carbon film was observed on a JEOL JEM 200-CX by applying a dark-field imaging mode, at a direct magnification of 2800 times. The minimum dose system was used to reduce the electron beam damage to the samples.[3] The electron microscope was operated with a 650 mm camera length at 200 kV in acceleration voltage. On the other hand, transferred multilayers were observed with a Hitachi TEM H-300 in a dark-field imaging mode, at a direct magnification of 3000 times.

The mono- and multilayer films transferred on the platinum film were folded into two with the lining inside. The fold edge was observed in the bright-field imaging mode at a direct magnification of 160000 (JEM 200-CX) or 70000 (TEM H-300) times to determine the film thickness directly.

RESULTS AND DISCUSSION

Sample Characterization

Figure 1 shows the IR spectra of CTD and CTO, together with that of the starting material, cellulose. These cellulose esters have strong absorption peaks (in cm^{-1}) at 2926 and 2853 (CH stretching), at 1466 (CH_2 bending), and at 1750 (C=O stretching), but they lack the absorption peak around 3500 (OH stretching). This means that the three OH groups of a glucose unit were almost perfectly capped with the ester groups, *i.e.*, $DS \cong 3$.

Quantitative estimation of *DS* values was made by means of ^1H NMR and elemental analyses. Figure 2 shows a ^1H NMR spectrum of CTD as an example. Each band was assigned as follows:

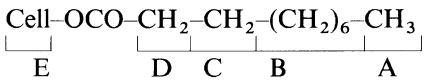

Using the integral values of the peak areas due to A (terminal methyl) and E (glucose ring), we calculated the *DS* value with the equation, $DS = 10A/(A+3E)$, to find $DS = 3.0$ for CTD. The same value was obtained also for CTO. Elemental analytical results were : for CTD, $C = 69.1_9$ (69.1_9) and $H = 10.4_9$ (10.3_2) and for CTO, $C = 75.2_2$ (74.9_5) and $H = 11.7_2$ (11.7_4) in percent. The values in parentheses were calculative for the formula $C_{36}H_{64}O_8$ and $C_{60}H_{112}O_8$, expected for CTD and CTO, respectively. These results also confirm a complete substitution for both cellulose esters.

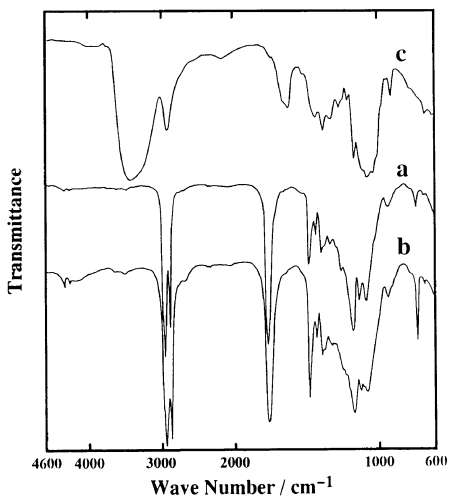

Figure 1. IR spectra of (a) CTD, (b) CTO, and (c) cellulose.

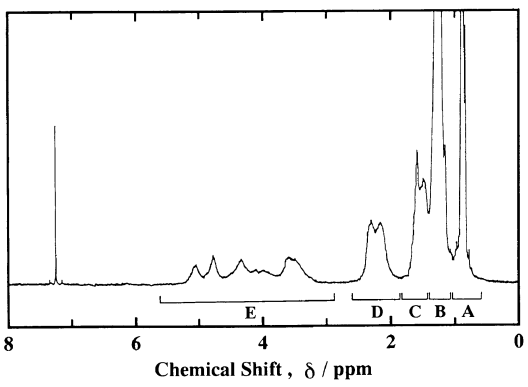

Figure 2. ^1H NMR spectrum of CTD in a $CDCl_3$ solution.

The π–A isotherms and Film Structure of CTD

Figure 3 shows the π–A isotherm of CTD spread from a benzene solution at 293 K. Its most remarkable feature is that the surface pressure π increases in two steps with decreasing area A, giving a plateau region for values of A roughly between 0.3 and 0.6 nm^2. This feature is believed to indicate a transition from a monolayer to a bilayer structure, as will be discussed later.

The isotherm reported by Kawaguchi *et al.*[4] for CTD ($DS=2.98$) spread from a chloroform solution (2×10^{-7} mol-eq in ml) is qualitatively similar to, but quantitatively very different from ours. In their isotherm, π begins to rise at about $A=1.4\,nm^2$ and the plateau region extends from about 0.6 to 1.1 nm^2. We have also made π–A measurements with chloroform and MIBK as solvents. The MIBK isotherm was substantially the same as the benzene curve reported above. The chloroform result is shown by the broken curve in Figure 3. (We have tried measurements at several different concentrations of the chloroform solution ranging from 1×10^{-7} to 1×10^{-6} mol-eq in ml, but the results were almost the same, and thus the curve given in Figure 3 may be considered as quite reproducible.) It can be seen that the chloroform curve is distinctly different from the benzene (and MIBK) curve. We presume that this difference may arise from the difference in the vaporization rates of the solvents: chloroform vaporizes perhaps too fast for the polymer molecules to attain a uniform distribution over the water surface. This could affect the π–A isotherm even at later stages, if a re-distribution of the molecules on the water, a non-solvent for them, is difficult to occur. Clearly, however, the observed difference is not as large as that between the chloroform isotherm of Kawaguchi *et al.* and the benzene isotherm of ours. We have no explanation for this. Insofar as our benzene curve is concerned, it can be interpreted consistently with the TEM results (see below). We also add that no qualitative difference was detectable by TEM between the benzene- and chloroform-spread films.

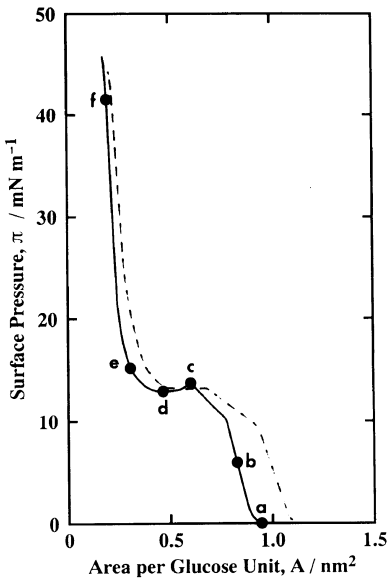

Figure 3. The π–A isotherm of CTD spread from a benzene solution at 293 K (solid line). Broken line : spread from a chloroform solution at 293 K. Points **a** to **f** denote where the monolayer was transferred. **a**, (π/mN m^{-1}, A/nm^2 glucose $unit^{-1}$)=(0, 0.95); **b**, (6, 0.83); **c**, (14, 0.59); **d**, (13, 0.46); **e**, (15, 0.30), **f** , (42, 0.19).

In the dark-field imaging mode of TEM, the objective aperture is shifted to block the main electron beam, admitting only those electrons scattered from the sample, and thus the sample film is observed as bright images in a dark background. The situation is reversed in the bright-field imaging mode.

Figures 4a to f show the dark- and the bright-field (inset) images of CTD films spread from the benzene solution and transferred at the six points correspondingly marked in Figure 3. At point **a**, where the isotherm is about to rise, many holes measuring 0.2—0.9 μm can be seen. The inset of Figure 4a shows that the film transferred at this point does not have a measurable thickness. At point **b**, the fraction of the holes has considerably decreased, and the film thickness measuring about 0.5 nm approximately equals that of a glucopyranose ring lying flat on a surface. At point

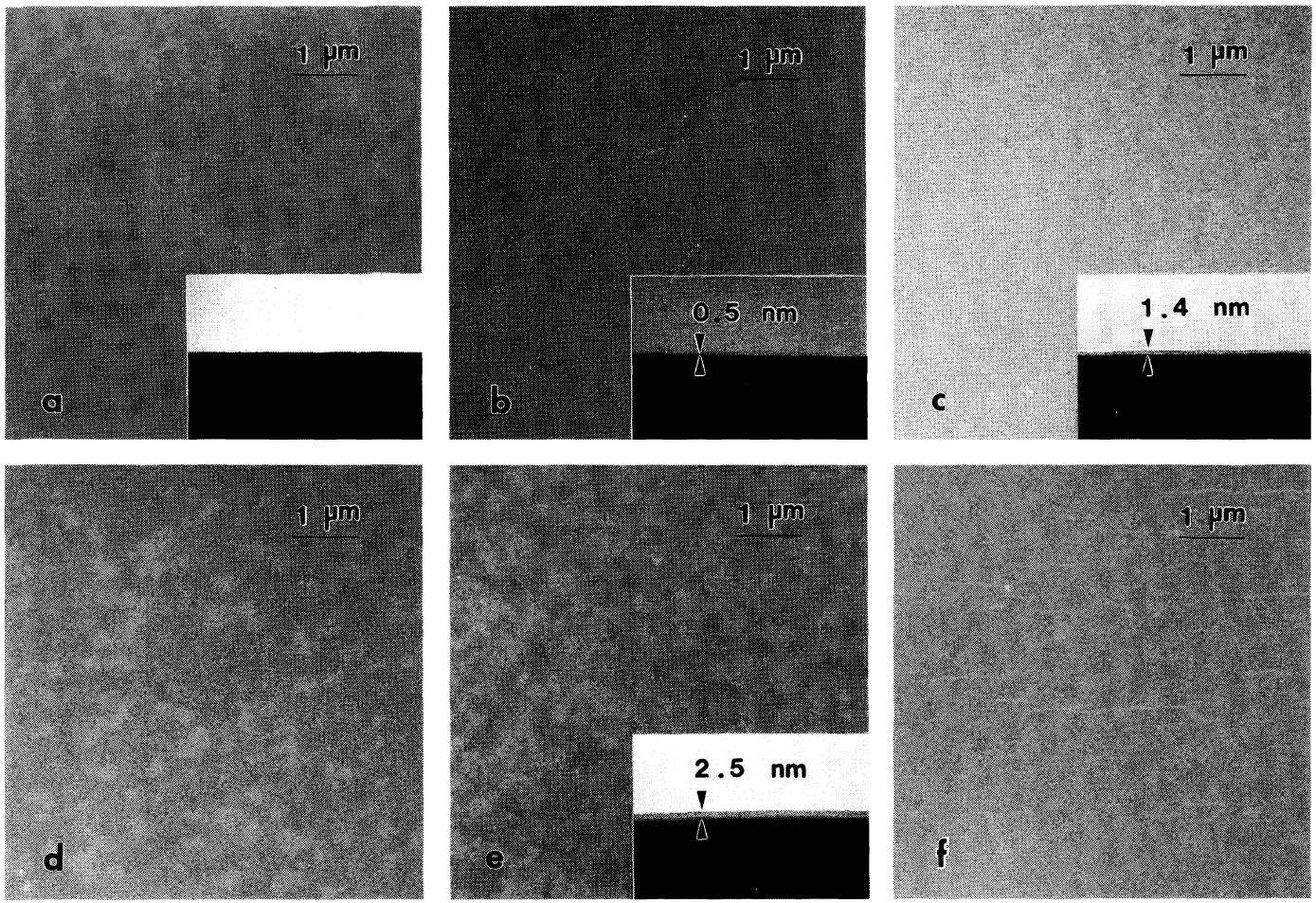

Figure 4. Dark- and bright-field (inset) images of CTD monolayer transferred at different points of the π–A isotherm as indicated in Figure 3.

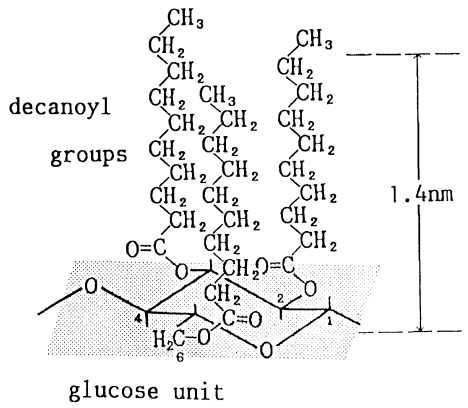

Figure 5. Schematic molecular model for the glucose unit of CTD at point **c** in Figure 3.

c, the film is seen to be *completely homogeneous*. The observed thickness is 1.4 nm, which is in good agreement with that of the molecular model for CTD depicted in Figure 5, where a glucopyranose ring lies flat on the water surface and the alkyl side chains, fully extended, stand normal to the glucopyranose ring. At point **d**, the film contains a number of starlike spots more or less uniformly distributed throughout the sight. At point **e**, the film is nearly entirely filled with starlike spots, and the film thickness measures 2.5 nm, nearly twice as thick as the monolayer. In addition, the area A at this point is 0.30 nm^2 per glucose unit, just a half of that at point **c**. At point **f**, the micrograph shows many shrinks indicating the collapse of the film.

On the basis of these observations, the following picture can be envisaged: as the monolayer of CTD spread at the air/water interface is compressed, the molecules which originally lie more or less flat on the surface come closer to each other, and beyond point **b**, the alkyl side chains begin to stand up on the surface. At point **c**, the side chains stand essentially normal to the water surface with the hydrophilic cellulose main chains lying essentially flat on the surface (Figure 5). The value of A at this point is 0.59 nm^2 per glucopyranose unit or 0.20 nm^2 per alkyl side chain, which favorably agrees with the cross-section of 0.18 nm^2 of a polymethylene chain in a polyethylene orthorhombic crystal. The observed film thickness, 1.4 nm, is also consistent with the assumed model. With a further compression, portions of the monolayer go on top of the remaining portions to form a monolayer/bilayer coexisting film, thus presenting the "starlike spots" appearance. (The molecular conformation in the bilayer structure, *i.e.*, Y-type *vs.* X-type, is presently unclear.) This "transition" process (except for its onset, where a small maximum can be seen in the π–A isotherm (Figure 3), and which will be discussed below) will be accompanied by essentially no increase of π, and hence the plateau region results. At point **e**, where A is just a half of that at point **c**, nearly the whole film becomes bilayered, as was confirmed by the dark-field image and the layer thickness. A further compression beyond this point brings about a steep rise of π, eventually leading to a collapsed film. The presence of an apparent plateau has also been noted for the π–A isotherms of poly(γ-methyl L-glutamate) and poly(γ-benzyl L-glutamate),[5] which has been claimed to reflect a monolayer–bilayer transition.

The above-noted maximum appearing at the onset of the transition is believed to be relevant to a potential barrier for the transition. When this barrier is too high, no transition to a bilayered structure would possibly occur. In fact, CTO, which has much longer side chains and hence is expected to have a larger barrier, forms only a monolayer structure throughout the compressing process (see below). Figure 6 compares the benzene-spread isotherms observed at different temperatures. They are quite the same, except for the plateau and collapsing regions. The maxima observed at low temperatures disappeared at 303 K. The decrease in the collapse pressure with increasing temperature seems to reflect a decrease in stability of the film due to increased mobilities of the sample and subphase molecules. We have attempted to characterize the transition in terms of a

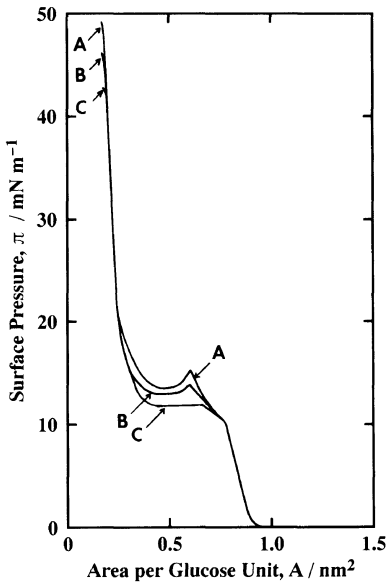

Figure 6. The π–A isotherms of CTD spread from a benzene solution at 283 K (A), 293 K (B), and 303 K (C).

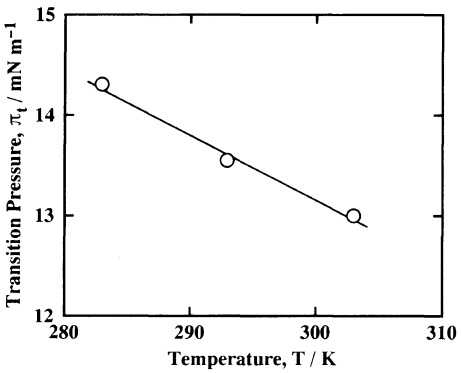

Figure 7. Temperature effect on π_t.

two-dimensional analogue of the Clausius–Clapeyron equation,

$$d\pi_t/dT = \Delta H/T\Delta A$$

Here, π_t is the equilibrium transition pressure at temperature T, and ΔA and ΔH are the net changes in molar area and molar enthalpy, respectively, accompanying the transition. As for the values of π_t and ΔA, the reading of π at the center of the plateau and the span in A of the plateau region were used. From the π_t *vs.* T plot shown in Figure 7, the slope of $d\pi_t/dT$ was estimated to be $-0.13\,\mathrm{mN\ (mK)^{-1}}$. ΔH was calculated to be $8.2\,\mathrm{kJ\,mol^{-1}}$ per glucose unit at 293 K. This ΔH value is about a half of that reported by Kawaguchi *et al.*,[4] who used chloroform as a spreading solvent. Since their value of $d\pi_t/dT$ is similar to ours, the difference in ΔH comes entirely from the difference in the span of the plateau, as already noted.

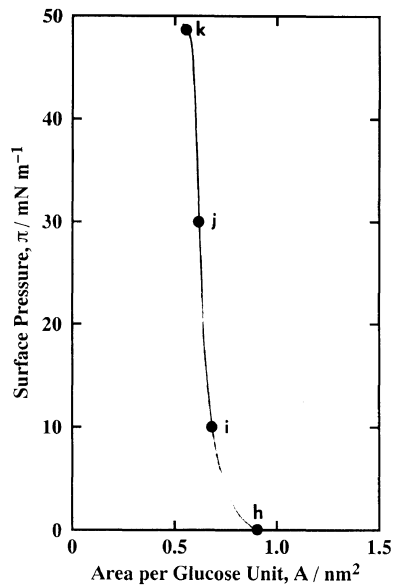

Figure 8. The π–A isotherm of CTO spread from a benzene solution at 293 K. Points **h** to **k** denote where the monolayer was transferred. **h**: (π/mN m^{-1}, A/nm^2 glucose unit^{-1}) = (0, 0.90); **i**, (10, 0.70); **j**, (30, 0.62); **k**, (49, 0.56).

The π–A isotherm and Monolayer Structure of CTO

Figure 8 shows the π–A isotherm of CTO spread from a benzene solution at 293 K. Unlike those of CTD , no plateau appears, as already mentioned: this polymer forms a condensed-type film at this temperature. This feature is similar to those of the films of stearic acid and of cellulose tri(*n*-hexadecanoate).[4] It follows that the length of alkyl chains has dominant effects on the surface properties. This may be interpreted in terms of the overall

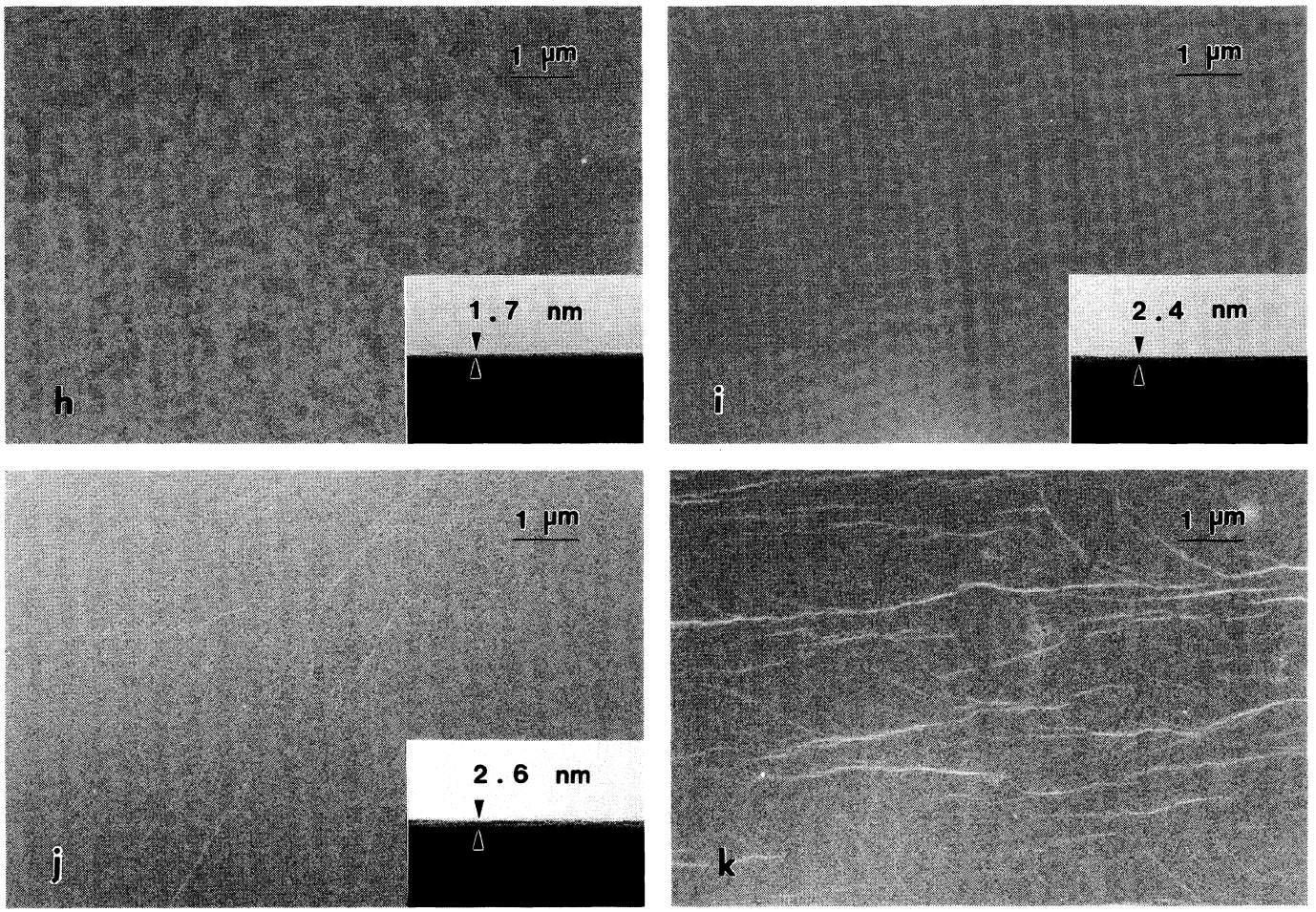

Figure 9. Dark- and bright-field images of CTO monolayers transferred at different points of the π–A isotherm as indicated in Figure 8.

cohesive force being dependent on the alkyl length.

Figure 9 shows the TEM images of CTO transferred at the four stages marked in Figure 8. At point **h**, the film is composed of large aggregates of different sizes (*ca.* 1 to 10 μm in diameter). At point **i**, the film is homogeneous, and its thickness measures 2.4 nm, somewhat smaller than the value 2.6 nm estimated from a model similar to that shown in Figure 5. At points **j** and **k**, distinct shrinks can be seen, showing that the monolayer has partially or largely collapsed. The molecular conformation in the CTO homogeneous film will be discussed in the next section.

Multilayer Structure of CTO

We have made various attempts to deposit the homogeneous CTO monolayer formed at a pressure $\pi = 10\,\mathrm{mN\,m^{-1}}$. The vertical dipping method along with the use of either the hydrophilic or hydrophobic substrates led to unsuccessful results. When the hydrophilic substrate was used, however, the first dipping-out process gave a successful deposition with a transfer ratio of unity, but trials of further deposition failed. Use of the hydrophobic substrate gave totally undesirable results. This is presumably because the substituted cellulosic backbone is not sufficiently hydrophilic and/or because the cellulosic chain lacks a sufficient flexibility.

The horizontal lifting method with the hydrophobic substrate gave successful results: Figure 10 shows the transfer ratio r as a function of the deposition number n, where r is the ratio, to the surface area of the substrate, of the decrease in the area of the surface monolayer as measured by the migration of the moving bar (at a constant surface pressure) before and after a deposition. A transfer ratio of unity indicates a successful deposition of the monolayer. The figure shows that the monolayer is always transferred with a constant transfer ratio of 2.0. Since in this method, there is no barrier around the plate, the built-up film

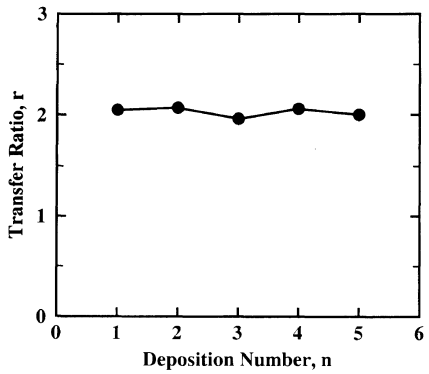

Figure 10. Transfer ratio for the hydrophobic plate (horizontal lifting method).

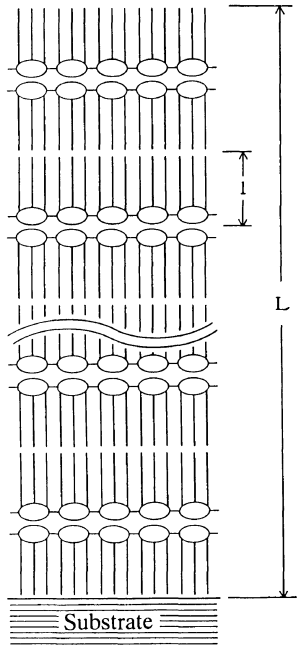

Figure 11. Schematic model for the CTO multilayer films.

will not be an X-type one that is obtained with the well-known cookie pattern with a Teflon frame.[11] When the plate is horizontally brought down to just touch the surface, the first layer will be deposited on it with the hydrophobic alkyl groups attached to the plate surface and the hydrophilic glucopyranosic groups appearing on the film surface. As the plate is brought up, the surrounding monolayer

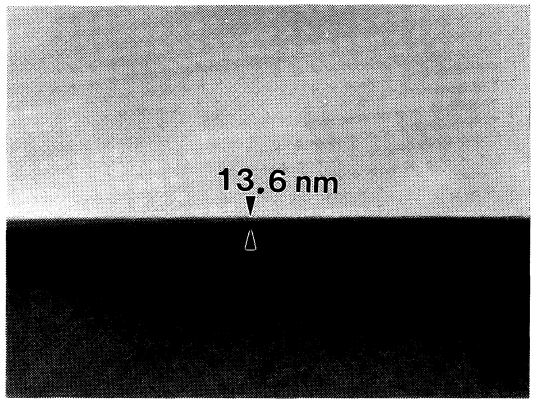

Figure 12. Bright-field image of the 6-layer film of CTO, observed at a direct magnification of 70000 times.

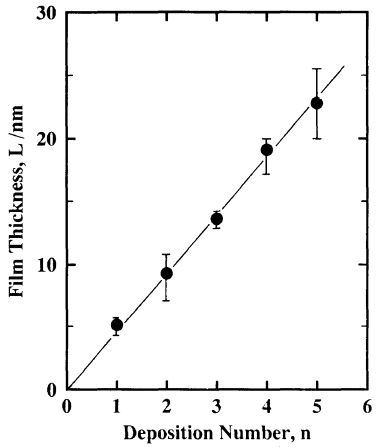

Figure 13. Film thickness L plotted against the number of deposition n.

will be drawn up, folded, and deposited on top of the first layer with the hydrophilic groups inside and the hydrophobic groups outside. Namely, a Y-type film is formed.[12,13] The constant transfer ratio of 2.0 observed for repeated depositions suggests a film structure such as illustrated in Figure 11, in which Y-type multilayer films are built up regularly. The deposition was equally successful with both the carbon-coated and the platinum-coated plates, which were used for the observations of the surface fine structure and the layer-thickness, respectively.

Figure 12 shows, as an example, the cross-section image of the 6-layer film obtained by the folding method. The film built up on the platinum base is clearly observed as a layer measuring 13.6 nm in thickness. In Figure 13, the thickness L thus measured is given as a function of the number of depositions, n. The figure shows that L is proportional to n, indicating that each layer is deposited regularly, confirming the model shown in Figure 11. From the slope of the line, the thickness per layer (half the slope) is calculated to be 2.3 nm, in good agreement with the above-noted thickness of the monolayer, 2.4 nm.

The observed thicknesses, however, are somewhat smaller than the value 2.6 nm expected for the molecular model (*cf.*, Figure 5). The mentioned difference between the observation and the model seems to parallel another observation that the limiting area per alkyl side chain is 0.23 nm^2, significantly larger than that of the CTD monolayer (0.20 nm^2) and the cross-section (0.18 nm^2) of the methylene chain in a polyethylene orthorhombic crystal. The difference may be interpreted either by a certain disorder of the conformation of the alkyl side chains or by a tilting of their chain axis. In this connection, we note that the CTO monolayer gave a distinct electron diffraction in a halow (the CTD monolayer gave no such clear diffraction, possibly because of the film being too thin). This halow corresponded to a real spacing of 0.46 nm, which, if the alkyl chains are assumed to be packed in a two-dimensional hexagonal order, corresponds to an occupied area of 0.22 nm^2 per chain, in favorable agreement with the value indicated by the limiting area. This suggests that the conformational disorder of the alkyl chains, if any is present, should not be too serious. In light of this result, the latter interpretation in terms of a tilting of the chain axis may sound more plausible. If this is correct, the tilt angle is estimated to be about 20 to 30° from the normal to the film surface.

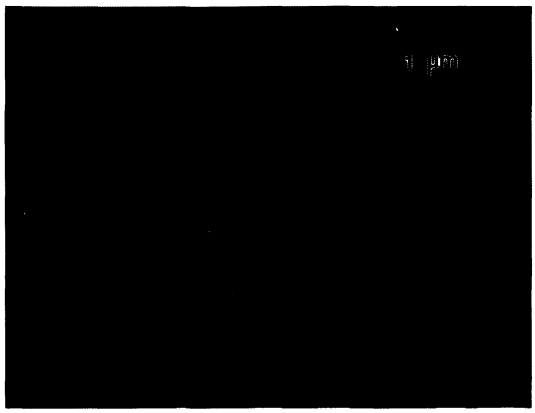

Figure 14. Dark-field image of the 10-layer film of CTO; observed at a direct magnification of 3000 times.

Figure 14 shows the dark-field image of the 10-layer film deposited at $\pi = 10\,\mathrm{mN\,m^{-1}}$. No characteristic texture can be observed. Thus the built-up film has a homogeneous surface structure. A preliminary result of a fluorescence spectroscopic study on a pyrene-labeled CTO suggests that there is no intermixing of the molecules belonging to different layers.[14] From all these, we believe that in the LB films of CTO, each layer is regularly accumulated with the alkyl side chains essentially extended, perhaps with the chain axis somewhat inclined against the film surface. The possibility of the existence of some conformational disorder within each layer cannot be ruled out, however.

Acknowledgments. This work was partially supported by a Grant-in-Aid for Scientific Research (No. 01490011) from the Ministry of Education, Science, and Culture of Japan. The authors thank Dr. M. Matsumoto and Dr. T. Kamata, Institute for Chemical Research, Kyoto University, for helpful discussions.

REFERENCES

1. (a) *Thin Solid Films*, **178–180** (1989). (b) *Thin Solid Films*, **159–160** (1988).
2. G. G. Roberts, *Adv. Phys.*, **34**, 475 (1985).
3. N. Uyeda, T. Takenaka, K. Aoyama, M. Matsumoto, and Y. Fujiyoshi, *Nature*, **327**, 319 (1987).
4. (a) T. Kawaguchi, H. Nakahara, and K. Fukuda, *J. Colloid Interface Sci.*, **104**, 290 (1985). (b) T. Kawaguchi, H. Nakahara, and K. Fukuda, *Thin Solid Films*, **133**, 29 (1985).
5. (a) F. Takeda, M. Matsumoto, T. Takenaka, and Y. Fujiyoshi, *Thin Solid Films*, **84**, 220 (1981). (b) T. Kawai, J. Umemura, and T. Takenaka, *Chem. Phys. Lett.*, **162**, 243 (1989).
6. M. Fujihira, K. Nishiyama, and H. Yamada, *Thin Solid Films*, **132**, 77 (1985).
7. (a) T. Itoh, H. Suzuki, M. Matsumoto, and T. Miyamoto, "Cellulose: Structural and Functional Aspects," J. F. Kennedy, G. O. Phillips, and P. A. Williams, Ed., Ellis Horwood, Chichester, 1989, p 409. (b) M. Matsumoto, T. Itoh, and T. Miyamoto, "Cellulosics Utilization," H. Inagaki and G. O. Phillips, Ed., Elsevier, London, 1989, p 151.
8. C. J. Malm, J. W. Mench, D. L. Kendall, and G. D. Hiatt, *Ind. Eng. Chem.*, **43**, 684 (1951).
9. R. C. Williams and R. M. Glaeser, *Science*, **175**, 1000 (1972).
10. Y. Harada, H. Hayashi, H. Ozaki, T. Kamata, J. Umemura, and T. Takenaka, *Thin Solid Films*, **178**, 305 (1989).
11. (a) K. Fukuda, H. Nakahara, and T. Kato, *J. Colloid Interface Sci.*, **54**, 430 (1976); (b) H. Nakahara and K. Fukuda, *ibid.*, **69**, 24 (1979).
12. (a) T. Kawai, J. Umemura, and T. Takenaka, Langmuir, 6, 672 (1990).
13. (a) M. Iwahashi, F. Naito, N. Watanabe, and T. Seimiya, *Chem. Lett.*, 187 (1985). (b) M. Iwahashi, F. Naito, N. Watanabe, T. Seimiya, N. Morikawa, N. Nogawa, T. Ohshima, H. Kawakami, K. Ukai, I. Sugai, S. Shibata, T. Yasuda, Y. Shoji, T. Suzuki, T. Nagafuchi, H. Taketani, T. Matsuda, Y. Fukushima, M. Fujioka, and K. Hisatake, *Bull. Chem. Soc. Jpn.*, **58**, 2093 (1985). (c) M. Iwahashi, K. Itoh, K. Ohshima, T. Seimiya, A. Yoshida, K. Kobayashi, and K. Takaoka, *ibid.*, **61**, 3061 (1988).
14. Y. Tsujii, T. Itoh, T. Fukuda, T. Miyamoto, S. Ito, and M. Yamamoto, *Langmuir*, **8**, 936 (1992).